Inorg. Chem. **2005**, *44*, 7970–7980

Reductive and Oxidative DNA Damage by Photoactive Platinum(II) Intercalators

Wei Lu, David A. Vicic,† and Jacqueline K. Barton*

Division of Chemistry and Chemical Engineering, California Institute of Technology, Pasadena, California 91125

Received July 6, 2005

Several photoactive platinum α-diimine intercalators have been prepared to develop new probes of DNA oxidation and reduction chemistry. Five water-soluble bis(mes′)Pt(II) complexes (mes′ = *N*,*N*,*N*,3,5-pentamethylaniline) with various aromatic α-diimine ligands (dppz = dipyridophenazine, np = naphtha[2,3-*f*][1,ω]phenanthroline, CN-np = naphtho[2,3-*f*][1,10]phenanthroline-9-carbonitrile, CN_2-np = naphtho[2,3-*f*][1,10]phenanthroline-9,14-dicarbonitrile, and bp = benzo-[*f*][1,10]phenanthroline) were synthesized. The complex $[(np)Pt(mes')_2]Cl_2$ was also characterized by X-ray crystallography, and the crystal structure shows that the *ortho*-methyl groups of the mes′ ligands conveniently block substitution at the vacant sites of platinum without overlapping with the intercalating α-diimine ligand. The Pt(II) complexes were found to have excited-state oxidation and reduction potentials of –0.6 to –1.0 and 1.0 to 1.5 V versus NHE, respectively, making them potent photoreductants as well as photooxidants. Many of the complexes are found to promote the photooxidation of N^2-cyclopropyldeoxyguanosine ($d^{Cp}G$). Photoexcited $[(dppz)Pt(mes')_2]^{2+}$ is found to be most efficient in this photooxidation, as well as in the photoreduction of N^4-cyclopropylcytidine (^{Cp}C); these modified nucleosides rapidly decompose in a ring-opening reaction upon oxidation or reduction. Photoexcited $[(dppz)Pt(mes')_2]Cl_2$, upon intercalation into the DNA π stack, is found, in addition, to promote reductive and oxidative damage within the DNA duplex, as is also probed using the kinetically fast electron and hole traps, ^{Cp}C and ^{Cp}G. These Pt complexes may therefore offer useful reactive tools to compare and contrast directly reductive and oxidative chemistry in double helical DNA.

Introduction

Metallointercalators have been extensively applied in probing oxidative DNA chemistry, but few experiments have been conducted with metal complexes to probe reductive reactions on DNA.[1] Indeed rhodium and ruthenium intercalators served as the first tethered probes of long-range oxidative DNA damage.[2,3] Recently, long-range reductive chemistry on DNA in solution has been demonstrated but only using tethered organic reductants.[4] We have been interested in developing metal complexes that could serve both as oxidative and reductive DNA probes, so that long-range electron and hole transfer through DNA might be examined and compared in parallel.

Platinum(II) α-diimine complexes are attractive candidates for reducing DNA because their excited states have large negative oxidation potentials and reasonably long lifetimes in fluid solution.[5] Indeed, some organometallic platinum complexes serve both as potent photooxidants and reductants;[6] also cyclometalated platinum complexes with planar heterocyclic ligands have been prepared that are highly luminescent and bind DNA avidly.[7] The excited-state oxida-

* To whom correspondence should be addressed. E-mail: jkbarton@caltech.edu.

† Present address: Department of Chemistry and Biochemistry, University of Arkansas, Fayetteville, AR 72701.

(1) Delaney, S.; Barton, J. K. *J. Org. Chem.* **2003**, *68*, 6475−6483.
(2) Hall, D. B.; Holmlin, R. E.; Barton, J. K. *Nature* **1996**, *382*, 731−735.
(3) Arkin, M. R.; Stemp, E. D. A.; Pulver, S. C.; Barton, J. K. *Chem. Biol.* **1997**, *4*, 389−400.
(4) (a) Giese, B.; Carl, B.; Carl, T.; Carell, T.; Behrens, C.; Hennecke, U.; Schieman, O.; Feresin, E. *Angew. Chem., Int. Ed.* **2004**, *43*, 1848−1851. (b) Breeger, S.; Hennecke, U.; Carell, T. *J. Am. Chem. Soc.* **2004**, *126*, 1302−1303. (c) Ito, T.; Rokita, S. E. *J. Am. Chem. Soc.* **2004**, *126*, 15552−15559. (d) Lewis, F. D.; Liu, X.; Miller, S. E.; Hayes, R. T.; Wasielewski, M. R. *J. Am. Chem. Soc.* **2002**, *124*, 11280−11281. (d) See also reductive chemistry on surfaces, for example: Kelley, S. O.; Jackson, N. M.; Hill, M. G.; Barton, J. K. *Angew. Chem., Int. Ed.* **1999**, *38*, 941−945.
(5) (a) Hissler, M.; McGarrah, J. E.; Connick, W. B.; Geiger, D. K.; Cummings, S. D.; Eisenberg, R. *Coord. Chem. Rev.* **2000**, *208*, 115−137. (b) Chan, S. C.; Chan, M. C. W.; Wang, Y.; Che, C. M.; Cheung, K. K.; Zhu, N. *Chem.—Eur. J.* **2001**, *7*, 4180−4190. (c) Whittle, C. E.; Weinstein, J. A.; George, M. W.; Schanze, K. S. *Inorg. Chem.* **2001**, *40*, 4053−4062.

10.1021/ic051124l CCC: $30.25
Published on Web 09/29/2005

tion potentials of some of these platinum complexes are high enough to reduce thymine or cytosine, with reduction potentials of ~−1.1 V versus NHE.[8] However, these platinum complexes, besides serving as potent photoreductants, require modification for interaction with DNA. First, the complexes need to be made water soluble and preferably positively charged to enhance electrostatic interactions with the DNA polyanion. Additionally, the aromatic diimine ligands should be extended so that the complexes can intercalate within the base stack of DNA.[9] We have found in studies of DNA-mediated photooxidation that intercalative stacking is preferred.[10] The extent of oxidative base damage has been shown to correlate with the strength of intercalative binding, and one may expect a similar trend with reductive base damage if the pathway to damage is through the base stack. Last, some protection of the platinum center may be required to limit direct covalent binding upon photoreaction because efficient photosubstitution reactions of platinum(II) complexes are common.

Reductive DNA chemistry is perhaps also more difficult to identify than DNA-mediated oxidative reactions. Long-range oxidative chemistry on DNA was able to be characterized in part because of the long lifetime and extensive irreversible reactions of the guanine radical,[2,3,11] the favored thermodynamic product of one-electron DNA oxidation.[12] Thymine dimer repair can be triggered both through oxidation and reduction,[4,13] and hence thymine dimers have provided a useful trap in establishing long-range DNA reactions. Because of the possibility of rapid back-electron transfer, another fast trap for oxidative and potentially reductive chemistry has been developed through modification of DNA bases with cyclopropylamine.[14−16] Upon oxidation or reduction, the cyclopropylamine moiety can undergo fast (10^{11} s^{-1}) ring opening to give an irreversible trap to report the reaction.

Here, we describe the preparation and characterization of a series of platinum complexes that may represent promising tools to probe reductive DNA chemistry. The cationic complexes bind noncovalently to DNA, and their excited-state potentials are sufficient to promote both oxidative and reductive DNA reactions. The ring-openings upon photoreaction of N^2-cyclopropyldeoxyguanosine ($d^{Cp}G$) and N^4-cyclopropylcytidine (^{Cp}C), both as free nucleosides and incorporated within the DNA duplex, are monitored as sensitive probes of oxidative and reductive chemistry. These platinum complexes are seen to promote efficient oxidation of $d^{Cp}G$ and reduction of ^{Cp}C and hence provide a new starting point for probing both oxidation and reduction chemistry on DNA in parallel.

Experimental Section

Synthesis. All starting materials were used as received, and all operations were performed under an argon atmosphere. ***Caution:*** *Organotin compounds are highly toxic and readily penetrate the skin.* Compounds *cis*-dichlorobis(dimethyl sulfoxide)platinum(II) [*cis*-$(dmso)_2PtCl_2$],[17] 4-bromo-*N*,*N*,3,5-tetramethylaniline,[18] 1,10-phenanthroline-5,6-dione (dipyridobenzoquinone, dpq),[19] dibenzo-[*a*,*c*]phenazine (dppz),[20] benzo-[*f*][1,10]phenanthroline (bp),[21] N^2-cyclopropyldeoxyguanosine,[16] and N^4-cyclopropylcytidine[16] were prepared according to literature methods. Oligonucleotides were synthesized utilizing standard phosphoramidite chemistry on an ABI 392 DNA/RNA synthesizer. DNA was synthesized with a 5′-dimethoxy trityl (DMT) protecting group and purified on a Dynamax 300 Å C_{18} reverse-phase column (Varian) (100% 50 mM NH_4OAc, pH 7.0, to 70% 50 mM NH_4OAc/ 30% acetonitrile over 35 min) on a Hewlett-Packard 1050 HPLC.

[(mes′)SnMe$_3$]BPh$_4$. *tert*-Butyllithium (1.7 M in pentane, 40 mL, 68.0 mmol) and, then, trimethyltin chloride (1.0 M in THF, 40 mL, 40 mmol) were added dropwise to a mixture of 4-bromo-*N*,*N*,3,5-tetramethylaniline bromine (9.5 g, 41.7 mmol) and TMEDA (5 mL) in THF (160 mL) at −78 °C under argon. The resulting suspension was stirred at −78 °C for 1 h, followed by stirring at ambient temperature for 1 h. Ether (200 mL) was added to the mixture, and the solution was washed twice with water. After the organic phase was dried with Na_2SO_4 and evaporated to dryness, the residue was washed with methanol, and the white solid of 4-trimethylstannyl-*N*,*N*,3,5-tetramethylaniline was collected on a sinter glass filter (yield 6.0 g, 47%). This solid was then dissolved in a minimum amount of THF, and MeI (5 equiv) was added. The mixture was stirred in the dark for 24 h, and then the solvents were removed under reduced pressure. The residue was dissolved in a minimum amount of MeOH, and solid $NaBPh_4$ (7 g) was added. A large amount of precipitate appeared, which was filtered and washed with methanol and ether. Yield: 11.9 g, 96%. ^{1}H NMR (300 MHz, dmso-d_6): δ 7.54 (s, 2H), 7.17 (br s, 8H), 6.91 (t, J = 7.2 Hz, 8H), 6.78 (t, J = 7.1 Hz, 4H), 3.51 (s, 9H), 2.45 (s, 6H), 0.37 (s with ^{119}Sn satellites, J_{SnH} = 54.4 Hz, 9H). Anal. Calcd for $C_{38}H_{46}BNSn$: C, 70.84; H, 6.88. Found: C, 70.88; H, 7.04.

[(dmso)$_2$Pt(mes′)$_2$](BPh$_4$)$_2$. The mixture of *cis*-$(dmso)_2PtCl_2$ (165 mg, 0.39 mmol) and [(mes′)$SnMe_3$]BPh_4 (520 mg, 0.80 mmol) in

(6) (a) Cummings, S. D.; Eisenberg, R. *J. Am. Chem. Soc.* **1996**, *118*, 1949−1960. (b) Hissler, M.; Connick, W. B.; Geiger, D. K.; McGarrah, J. E.; Lipa, D.; Lachicotte, R. J.; Eisenberg, R. *Inorg. Chem.* **2000**, *39*, 447−457. (c) Wadas, T. J.; Lachicotte, R. J.; Eisenberg, R. *Inorg. Chem.* **2003**, *42*, 3772−3778. (d) Dungey, K. E.; Thompson, B. D.; Kane-Maguire, N. A. P.; Wright, L. L. *Inorg. Chem.* **2000**, *39*, 5192−5196.

(7) (a) Liu, H. Q.; Peng, S. M.; Che C. M. *J. Chem. Soc., Chem. Commun.* **1995**, 509−510. (b) Che, C. M.; Yang, M. S.; Wong, K. H.; Chan, H. L.; Lam, W. *Chem.—Eur. J.* **1999**, *5*, 3350−3356. (c) Ma, D. L.; Che, C. M. *Chem.—Eur. J.* **2003**, *9*, 6133−6144.

(8) (a) Steenken, S.; Telo, J. P.; Novais, H. M.; Candeias, L. P. *J. Am. Chem. Soc.* **1992**, *114*, 4701−4709. (b) Steenken, S.; Jovanovic, S. V. *J. Am. Chem. Soc.* **1997**, *119*, 617−618.

(9) (a) Erkkila, K. E.; Odom, D. T.; Barton, J. K. *Chem. Rev.* **1999**, *99*, 2777−2795. (b) Kielkopf, C. L.; Erkkila, K. E.; Hudson, B. P.; Barton, J. K.; Rees, D. C. *Nat. Struct. Biol.* **2000**, *7*, 117−121.

(10) Delaney, S.; Pascaly, M.; Bhattacharya, P. K.; Han, K.; Barton, J. K. *Inorg. Chem.* **2002**, *41*, 1966−1974.

(11) Williams, T. T.; Dohno, C.; Stemp, E. D. A.; Barton, J. K. *J. Am. Chem. Soc.* **2004**, *126*, 8148−8158.

(12) Sugiyama, H.; Saito, I. *J. Am. Chem. Soc.* **1996**, *118*, 7063−7068.

(13) Dandliker, P. J.; Holmlin, R. E.; Barton, J. K. *Science* **1997**, *275*, 1465−1468.

(14) Nakatani, K.; Dohno, C.; Saito, I. *J. Am. Chem. Soc.* **2001**, *123*, 9681−9682.

(15) (a) Williams, T. T.; Dohno, C.; Stemp, E. D. A.; Barton, J. K. *J. Am. Chem. Soc.* **2004**, *126*, 8148−8158. (b) O'Neill, M. A.; Dohno, C.; Barton, J. K. *J. Am. Chem. Soc.* **2004**, *126*, 1316−1317.

(16) Shao, F. W.; O'Neill, M. A.; Barton, J. K. *Proc. Natl. Acad. Sci. U.S.A.* **2004**, *101*, 17914−17919.

(17) Kukushkin, V. Y.; Pombeiro, A. J. L.; Ferreira, C. M. P.; Elding, L. I.; Puddephatt, R. J. *Inorg. Synth.* **2002**, *33*, 189−196.

(18) Engman, L.; Stern, D.; Stenberg, B. *J. Appl. Polym. Sci.* **1996**, *59*, 1365−1369.

(19) Paw, W.; Eisenberg, R. *Inorg. Chem.* **1997**, *36*, 2287−2293.

(20) Dupureur, C. M.; Barton, J. K. *Inorg. Chem.* **1997**, *36*, 33−43.

(21) Do, C. T.; Jacquignon, P.; Dufour, M. *J. Heterocyclic Chem.* **1976**, *13*, 641−644.

DMSO (4 mL) was heated at 95 °C for 24 h. After the mixture was cooled to ambient temperature, methanol and diethyl ether were added to precipitate $[(dmso)_2Pt(mes')_2](BPh_4)_2$ as a white solid which was washed with methanol and ether. Yield: 320 mg, 63%. ^{1}H NMR (300 MHz, CD_3CN): δ 7.35 (s, 4H), 7.13 (br s, 16H), 6.88 (t, $J = 7.8$ Hz, 16H), 6.75 (t, $J = 7.8$ Hz, 8H), 3.48 (s, 18H), 2.69 (s, 12H), 2.68 (s, 12H). Anal. Calcd for $C_{74}H_{86}B_2N_2O_2PtS_2$: C, 67.53; H, 6.58. Found: C, 67.13; H, 6.41.

Naphtho[2,3-*f*][1,10]phenanthroline-9,14-dicarbonitrile, CN_2-np. This compound was prepared using a modified literature method.[22] DBU (1.5 mL) was added to a mixture of dipyridobenzoquinone (2.0 g, 9.5 mmol) and 1,2-phenylenediacetonitrile (1.7 g, 10.9 mmol) in CH_3CN (60 mL), and the solution was refluxed for 30 min. The suspension was then cooled to ambient temperature, and the precipitate was collected by filtration and washed with CH_3CN. Yield: 2.0 g, 64%. ^{1}H NMR (300 MHz, $CDCl_3$): δ 9.85 (d, $J = 8.4$ Hz, 2H), 9.25 (br s, 2H), 8.69 (br s, 2H), 7.99 (br s, 2H), 7.78 (br s, 2H).

Naphtho[2,3-*f*][1,10]phenanthroline-9-carbonitrile, CN-np. The mixture of CN_2-np (1.0 g) and KOH (6.0 g) in ethanol (200 mL) was stirred at 40 °C for 2 days, and the resulting suspension was filtered. The red filtrate was refluxed for 24 h, and the solid was then filtered out and washed with water. The residue was extracted with CH_2Cl_2/CH_3OH (4/1, v/v) and the solution was filtered and evaporated to dryness to give a product (50 mg) which was used without further purification. EIMS: 307 ($M^+ + 2H$).

Naphtho[2,3-*f*][1,10]phenanthroline, np.[22] A mixture of dpq (2.0 g, 9.5 mmol) and *o*-xylylenebis(triphenylphosphonium bromide) (8.0 g, 10.1 mmol) in CH_2Cl_2 (100 mL) was added to an aqueous solution of LiOH (5 M, 5 mL), and the suspension was sonicated for 2 h. The suspension was then filtered and extracted twice with CH_2Cl_2. The organic phase was evaporated to dryness. The desired product was obtained as pale yellow needles after flash chromatography on silica gel (eluent, hexane/ethyl acetate = 1/5). Yield: 50 mg, 2%.

General Procedure for Synthesis of the Complexes. The respective α-diimine ligand (0.04 mmol) was added to $[(dmso)_2Pt(mes')_2](BPh_4)_2$ (44 mg, 0.03 mmol) in DMF (2 mL), and the mixture was heated at 95 °C for 4 h. The resulting solution, after cooling, was loaded onto an anion-exchange column (Sephadex QAE A-25 preequilibrated with Et_4NCl) and eluted with water/CH_3CN (1/1). The crude product was purified using flash chromatography on silica gel (eluent, CH_3CN, followed by water/CH_3CN 1/100) to give a yellow or brown powder after lyophilization.

[(dppz)Pt(mes')$_2$]Cl$_2$ (1). Yield: 13 mg, 45%. ^{1}H NMR (300 MHz, dmso-d_6): δ 9.12 (d, $J = 7.8$ Hz, 2H), 8.36 (d, $J = 5.4$ Hz, 2H), 7.96−7.85 (m, 4H), 7.73 (dd, $J = 7.8$ Hz, $J = 5.1$ Hz, 2H), 7.38 (s, 4H), 3.69 (s, 18H), 2.47 (s, 12H). FABMS: *m*/*z* 803.3266 (M^+), 839.2941 ($M^+ + Cl$), 788.3100 ($M^+ - CH_3$); calculated mass for M^+, 803.3276.

[(np)Pt(mes')$_2$]Cl$_2$ (2). Yield: 18 mg, 75%. ^{1}H NMR (300 MHz, dmso-d_6): δ 9.79 (d, $J = 7.8$ Hz, 2H), 9.67 (s, 2H), 8.32 (dd, $J = 5.7$ Hz, $J = 4.3$ Hz, 2H), 8.19 (d, $J = 5.7$ Hz, 2H), 8.03 (dd, $J = 7.8$ Hz, $J = 5.3$ Hz, 2H), 7.78 (dd, $J = 5.6$ Hz, $J = 4.3$ Hz, 2H), 7.30 (s, 4H), 3.54 (s, 18H), 2.55 (s, 12H). FABMS: *m*/*z* 801.3374 (M^+), 837.3146 ($M^+ + Cl$), 786.3255 ($M^+ - CH_3$); calculated mass for M^+, 801.3370.

[(CN-np)Pt(mes')$_2$]Cl$_2$ (3). Yield: 10 mg, 41%. ^{1}H NMR (300 MHz, CD_3CN): δ 10.07 (d, $J = 8.1$ Hz, 1H), 9.23 (m, 2H), 8.26 (m, 2H), 7.94 (m 2H), 7.83 (m 2H), 7.61 (m 2H), 7.23 (s, 4H), 3.81 (s, 18H), 2.66 (s, 12H). FABMS: *m*/*z* 826.3327 (M^+), 811.3106 ($M^+ - CH_3$); calculated mass for M^+, 826.3323.

[(CN$_2$-np)Pt(mes')$_2$]Cl$_2$ (4). Yield: 16 mg, 63%. ^{1}H NMR (300 MHz, dmso-d_6): δ 10.22 (d, $J = 7.7$ Hz, 2H), 8.67 (broad d, 2H), 8.33 (broad d, 2H), 8.18 (broad m, 4H), 7.33 (s, 4H), 3.55 (s, 18H), 2.48 (s, 12H). FABMS: *m*/*z* 851.3287 (M^+), 887.3299 ($M^+ + Cl$), 836.2964 ($M^+ - CH_3$); calculated mass for M^+, 851.3276.

[(bp)Pt(mes')$_2$]Cl$_2$ (5). Yield: 18 mg, 80%. ^{1}H NMR (300 MHz, dmso-d_6): δ 9.72 (d, $J = 8.1$ Hz, 2H), 9.04 (dd, $J = 6.3$ Hz, $J = 3.6$ Hz, 2H), 8.24 (d, $J = 5.1$ Hz, 2H), 8.05−7.97 (m, 4H), 7.30 (s, 4H), 3.53 (s, 18H), 2.54 (s, 12H). FABMS: *m*/*z* 751.3174 (M^+), 787.3492 ($M^+ + Cl$), 736.3074 ($M^+ - CH_3$); calculated mass for M^+, 751.3214.

Cyclic Voltammetry. Ground-state oxidation and reduction potentials for metal complexes were obtained on a CH Instruments Electrochemical Workstation. A glassy carbon working electrode, an Ag/AgCl reference electrode, and a Pt auxiliary electrode were used in a single-cell sample apparatus. Solutions of metal complex (~1 mM) in dry acetonitrile containing 0.1 M tetrabutylammonium hexafluorophosphate were degassed with argon prior to use, and voltammograms were collected using a 100 mV/s scan rate. $E_{1/2}$ values were taken as the average of the voltage of maximum current for the forward and reverse electrochemical processes. Ferrocene, as an internal standard, was added at the end of the measurements, and the potentials are reported in volts versus NHE ($Cp_2Fe^{+/0}$ = 0.66 V versus NHE).

Glassy Solution Emission Spectra. E_{0-0} data of the platinum(II) complexes were estimated from the 0−0 band in the structured emission spectra of these complexes in glassy 10 M LiCl solutions (complex concentrations $\approx 1 \times 10^{-5}$ M; $\lambda_{ex} = 350$ nm) at 77 K on a ISS K2 multifrequency phase fluorometer. Both excitation and emission data were examined.

Determination of Binding Constants to DNA. Absorption titrations on an HP 8452A Diode Array UV−vis spectrometer were performed to determine the affinity constants for metal complexes with the duplex of 3′-TACCATGTTCGACTAGACTC-5′ and its complementary strand. The DNA 20-mer, ranging from 0 to 1500 μM in base pairs, was titrated into solutions containing 20 μM metal complex, 20 mM sodium phosphate, 50 mM NaCl, pH 7.0. The intrinsic binding constants, *K*, were derived from a plot of $D/\Delta\epsilon_{ap}$ versus *D* according to eq 1[23]

$$D/\Delta\epsilon_{ap} = D/\Delta\epsilon + 1/(\Delta\epsilon K) \quad (1)$$

where *D* is the concentration of DNA in base pairs, $\Delta\epsilon_{ap} = |\epsilon_A - \epsilon_F|$ and $\Delta\epsilon = |\epsilon_B - \epsilon_F|$, the apparent extinction coefficient, $\epsilon_A = A_{obs}/[complex]$, ϵ_B and ϵ_F are the extinction coefficients of the bound and free form of the platinum(II) complex, respectively. The slope and *y* intercept of the linear fit of $D/\Delta\epsilon_{ap}$ versus *D* give $1/\Delta\epsilon$ and $1/(\Delta\epsilon + K)$, respectively.

X-ray Structural Determination of Single-Crystal [(np)Pt(mes')$_2$]Cl$_2$·(DMF)$_3$·(H$_2$O)$_2$. The slow diffusion of diethyl ether into a DMF solution of $[(np)Pt(mes')_2]Cl_2$ led to the formation of yellow plates. A single crystal of dimensions 0.30 × 0.19 × 0.07 mm^3 was mounted on a glass fiber in oil. Data were collected at 98 K on a Bruker SMART 1000 area detector running SMART version 5.054 and employing graphite-monochromated Mo Kα radiation with $\lambda = 0.71073$ Å.[24] Laue symmetry revealed a triclinic space group, and the cell parameters were determined from 11473 unique reflections. The space group was assigned as $P\bar{1}$ on the basis

(22) Albano, G.; Belser, P.; De Cola, L.; Gandolfi, M. T. *Chem. Commun.* **1999**, 1171−1172.

(23) Wolfte, A.; Shimer, G. H., Jr.; Meehan, T. *Biochemistry* **1987**, *26*, 6392−6396.

(24) *SMART*, *SAINT*, and *SHELXTL*; Bruker AXS Inc.: Madison, WI, 1999.

Scheme 1. Synthesis of Platinum Complexes

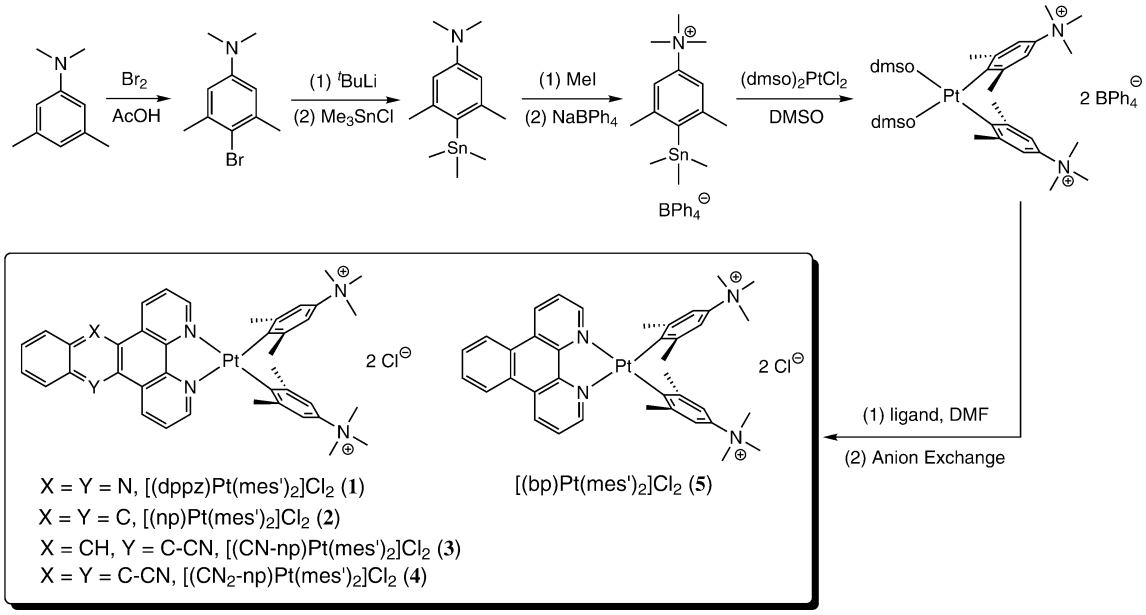

of systematic absences using XPREP, and the structure was refined using the SHELXS-97 package. In the final model, non-hydrogen atoms were refined anisotropically (full matrix on F^2), with hydrogens included in idealized locations. The structure refined with final residuals of R1 = 0.0391 and wR2 = 0.0634. The final structure also includes three DMF molecules and two water molecules. Fractional coordinates and thermal parameters are given in the Supporting Information.

Photoreactions with Nucleosides. For $d^{Cp}G$ photooxidation, a 30 μL aliquot of 20 μM Pt(II) complex and 20 μM $d^{Cp}G$ in 20 mM sodium phosphate, 50 mM NaCl, pH 7.0, was irradiated using a HgXe lamp for up to 20 min at 370 nm (~12.5 mW) for complexes **1**−**4** and 330 nm (~9 mW) for complex **5**. For ^{Cp}C photoreduction, a 30 μL aliquot of 500 μM Pt(II) complex and 500 μM ^{Cp}C in 20 mM sodium phosphate, 50 mM NaCl, pH 7.0, was irradiated using a HgXe lamp for up to 60 min at 370 nm (~12.5 mW) for complexes **1**−**4** and 330 nm (~9 mW) for complex **5**. After irradiation, 50 μL of water was added to each of the aliquots, and the resulting mixtures were analyzed by HPLC (Chemcobond 5-ODS-H, C_{18}, 4.6 × 150 mm^2; elution with 98% 50 mM NH_4OAc/2% acetonitrile to 86% 50 mM NH_4OAc/14% acetonitrile over 30 min with a flow rate of 1 mL/min).

Photoreactions with Oligonucleotides. DNA oligonucleotides were prepared by standard solid-phase synthesis, and cyclopropylamine modifications were incorporated as described previously.[15,16] DNA duplexes were prepared by mixing equimolar amounts of modified and $d^{CP}G$/$d^{CP}C$-containing strands to a final concentration of 5 μM and annealing in 20 mM sodium phosphate, 50 mM NaCl, pH 7.0. Melting temperatures of the various duplexes were seen to differ by ≤4 °C, indicating little destabilization by the cyclopropyl-modified bases. Where applicable, three freeze−pump−thaw cycles were applied to degas the 30 μL aliquot in an airtight cell. Samples were irradiated for up to 60 min at the wavelengths of 370 nm for complexes **1**−**4** and 330 nm for complex **5**. After irradiation, samples were fully digested with a mixture of alkaline phosphatase (33 units/mL), snake venom phosphodiesterase (3 units/mL), and nuclease P1 (33 units/mL) at 37 °C for 4.5 h and at 25 °C for 12 h. Digested solutions were analyzed by HPLC (Chemcobond 5-ODS-H, C_{18}, 4.6 × 150 mm^2; elution with 98% 50 mM NH_4OAc/2% acetonitrile to 86% 50 mM NH_4OAc/14% acetonitrile over 30 min with a flow rate of 1 mL/min).

Results and Discussion

Synthesis of Platinum(II) Complexes. Since the best method available for attaching two mesitylene ligands to a platinum center employs trialkyl(mesityl)tin reagents,[25,26] we focused our efforts on preparing an aryl stannane to deliver a ligand that could be rendered water soluble. Including an amine functionality in the mesitylene was therefore attractive, since the amine could be quaternized in a later step to provide a cationic ligand that had favorable electrostatic interactions with the negatively charged backbone of DNA. The ligand synthesis in Scheme 1 begins with lithiation of 4-bromo-*N*,*N*,3,5-tetramethylaniline in the presence of Me_3SnCl to form the functionalized tin reagent 4-trimethylstannyl-*N*,*N*,3,5-tetramethylaniline which can be isolated as an off-white solid simply by washing with cold methanol. The quaternary amine **[**(mes′)$SnMe_3$]I is formed by the addition of methyl iodide, and the resulting iodide salt can be converted to the tetraphenylborate salt [(mes′)$SnMe_3$]BPh_4 by addition of $NaBPh_4$ in methanol. Conversion to the tetraphenylborate salt is useful in rendering subsequent platinum complexes such as [$(dmso)_2$Pt(mes′)$_2$]$(BPh_4)_2$ more soluble in traditional organic solvents. The [$(dmso)_2$Pt(mes′)$_2$]-$(BPh_4)_2$ complex is formed by the addition of excess [(mes′)-$SnMe_3$]BPh_4 to a suspension of $(dmso)_2PtCl_2$ in dmso and heating the resulting mixture at 95 °C for 24 h. The [$(dmso)_2$Pt(mes′)$_2$]$(BPh_4)_2$ complex is a very useful precursor to a variety of platinum complexes because the dmso ligands can be easily replaced by traditional ligands such as α-diimines.

For this study, we were particularly interested in comparing the reactivity of Pt(mes′)$_2$ complexes containing α-diimines ligands with various redox potentials and π surfaces

(25) Eaborn, C.; Kundu, K.; Pidcock, A. *J. Chem. Soc., Dalton Trans.* **1981**, 933−938.
(26) Klein, A.; Kaim, W. *Organometallics* **1995**, *14*, 1176−1186. (b) Fees, J.; Ketterle, M.; Klein, A.; Fiedler, J.; Kaim, W. *J. Chem. Soc., Dalton Trans.* **1999**, 2595−2999.

(i.e., dppz, np, CN-np, CN_2-np and bp ligands); dppz was chosen because of its ability to intercalate between the base pairs of DNA.[27] The np complex was also targeted because the ligand was found to be 750 mV more difficult to reduce in the ground state than dppz.[22] Cyano-substituted np ligands were included additionally to provide a range of redox potentials. The bp complex has a relatively smaller π-conjugated ligand that could prevent it from deep intercalation into the DNA π stack.

All the new platinum diimine complexes are made by heating a DMF solution of $[(dmso)_2Pt(mes')_2](BPh_4)_2$ in the presence of the various diimine ligands (Scheme 1). After anion exchange, flash column chromatography, and lyophilization, all these platinum(II) complexes were isolated as their water-soluble dichloride salts. X-ray quality single crystals of **2** were obtained from slow diffusion of diethyl ether into a DMF solution containing **2**.

X-ray Structure of $[(np)Pt(mes')_2]Cl_2 \cdot (DMF)_3 \cdot (H_2O)_2$. The structure of $[(np)Pt(mes')_2]^{2+}$ is shown in Figure 1, and the crystal data are listed in Table 1. The bond lengths and angles (Supporting Information) around the Pt(II) center are comparable to those reported for other bis(mesityl)Pt(II) structures.[26] Nevertheless, the solid state structure provides intimate details about the environment of the platinum center. As one can see from the ORTEP diagram, the methyl substituents of the mes′ ligands block the axial sites of platinum, preventing further coordination at the vacant sites. Positioning the methyl groups from the mes′ ligands over the axial sites should not only prevent cross-linking of the platinum to any of the exocyclic amines of the DNA bases[28] but should also prevent any unwanted photosubstitutions from occurring. Similar mesitylene ligands are well-known to shield the axial sites on platinum complexes and prevent reactions, such as oxidative addition, that normally occur with ease at platinum diimine metal centers.[26]

It is noteworthy that there is partial overlap between the two planar np ligands of the adjacent complex molecules in a head-to-tail fashion in the crystal, as also shown in Figure 1, and the interplanar distance is about 3.5 Å, falling in the range for typical π-interaction distances.[29] This structural feature suggests that these Pt(II) complexes may aggregate through π interactions between the planar diimine ligands. It is interesting that the bulky 2,6-dimethyl groups still allow the planar diimine moieties to interact within a π stack, while shielding the Pt(II) center from nucleophilic attack; a similar arrangement might be expected for the complex intercalated in DNA.

Absorption Spectra. The salient features in the UV−vis absorption spectra of complexes **1**−**5** (Figure 2) are the modest bands in the range of 320−400 nm and the tails

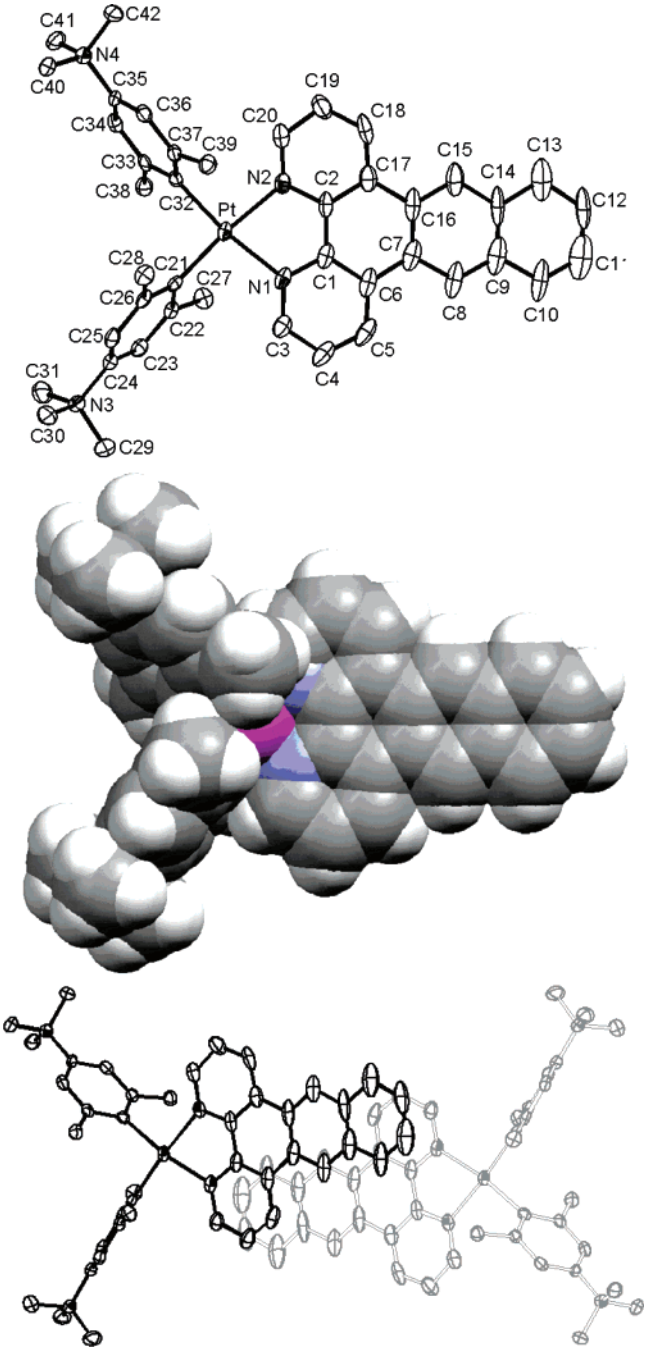

Figure 1. Perspective view with thermal ellipsoids at 50% probability (top), space-filling view (middle), and crystal-packing view (bottom) along *c* axis of the molecular structure of $[(np)Pt(mes')_2]Cl_2$ (**2**). The chloride ions, solvated water molecules, and DMF molecules are omitted for clarity.

beyond 450 nm that are tentatively assigned to the singlet and triplet [5d(Pt) → diimine] MLCT transitions, respectively. Little solvatochromic shift is seen for these bands when changing solvent, presumably because the mes′ ligands block the platinum center from interactions. However, the absorption intensity at 340 nm for the np complex is found to decrease by 56% from pure acetonitrile to pure aqueous solution. The dppz complex shows a similar effect, with an absorbance intensity drop of 42% in water versus acetonitrile. These drops in intensity are most likely the result of aggregation in the aqueous solution. It has been shown that the structural deviation in ligand−ligand, Pt···Pt, or both

(27) (a) Friedman, A. E.; Chambron, J. C.; Sauvage, J. P.; Turro, N. J.; Barton, J. K. *J. Am. Chem. Soc.* **1990**, *112*, 4960−4962. (b) Holmlin, R. E.; Stemp, E. D. A.; Barton, J. K. *Inorg. Chem.* **1998**, *37*, 29−34. (c) Hartshorn, R. M.; Barton, J. K. *J. Am. Chem. Soc.* **1992**, *114*, 5919−5925. (d) Onfelt, B.; Lincoln, P.; Norden, B. *J. Am. Chem. Soc.* **2001**, *123*, 3630−3637.
(28) Manchanda, R.; Dunham, S. U.; Lippard, S. J. *J. Am. Chem. Soc.* **1996**, *118*, 5144−5145.
(29) Lu, W.; Chan, M. C. W.; Cheung, K. K.; Che, C. M. *Organometallics* **2001**, *20*, 2477−2486.

Table 1. Crystal Data of $[(np)Pt(mes')_2]Cl_2 \cdot (DMF)_3 \cdot (H_2O)_2$

empirical formula	$C_{42}H_{46}N_4PtCl_2 \cdot (C_3H_7NO)_3 \cdot (H_2O)_2$	fw	1128.14
cryst color	yellow	cryst size (mm^3)	$0.30 \times 0.19 \times 0.07$
wavelength (Å)	0.71073 (Mo Kα)	temp (K)	98(2)
cryst syst	triclinic	space group	$P\bar{1}$
a (Å)	12.3592(9)	α (deg)	91.0060(10)
b (Å)	15.0644(11)	β (deg)	105.7790(10)
c (Å)	15.0726(11)	γ (deg)	112.0910(10)
D_c ($g\ cm^{-3}$)	1.511	V ($Å^3$)	2479.6(3)
Z	2	$F(000)$	1156
μ (mm^{-1})	2.991	$2\theta_{max}$ (deg)	56.9
no. reflns	51207	no. independent reflns	11473 [$R_{int} = 0.0571$]
no. variables	151	GOF on F^2	1.441
R1	0.0391	wR2	0.0634
residual ρ ($e\ Å^{-3}$)	+2.338, −2.085		

contacts leads to dramatic spectral changes,[30] but any Pt···Pt interactions can be ruled out in this case because of the bulky nature of the mes′ ligands. Instead, stacking of the hydrophobic diimine ligands through $\pi-\pi$ interactions appears to be the likely cause of the hypochromic effects. Indeed, in the solid state, the np ligands of **2** are found to pack in a stacked arrangement (vide supra).

Further evidence for the aggregation of these complexes in aqueous solution comes from the unusual spectral changes

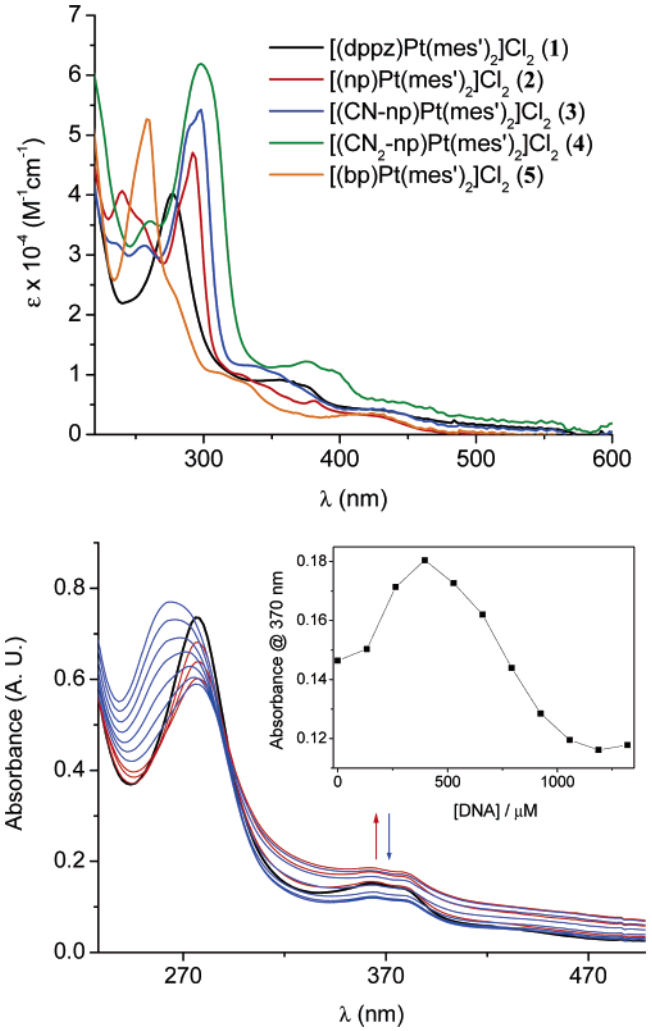

Figure 2. Absorption spectra of the complexes. UV−vis absorption spectra of complexes **1**−**5** in acetonitrile at ambient temperature (top). Absorption traces of the titration of a 20-mer DNA into 20 μM $[(dppz)Pt(mes')_2]Cl_2$ (**1**) in 20 mM sodium phosphate, 50 mM NaCl, pH 7.0 (bottom). The inset shows a plot of the absorbance at 370 nm vs the amount of DNA added.

observed as DNA is titrated into solutions containing the metal complexes. Figure 2 also shows the changes in absorption for **1** upon the addition of the duplex 3′-TACCATGTTCGACTAGACTC-5′. Initially, the absorbance intensities increase, as indicated by the red lines in Figure 2. Then, upon a further increase in the DNA concentration, the usual hypochromic shifts are observed (blue lines in Figure 2), consistent with intercalative stacking into DNA. A similar effect is observed for complexes **2**−**4** (Supporting Information) and has also been seen for the bulky $[Ru(bpy)_2(tpqp)]Cl_2$ (tpqp = 7,8,13,14-tetrahydro-6-phenylquino-[8,7-*k*][1,8]phenanthroline) complex.[31] An attractive explanation for this behavior is that when DNA is initially added, the aggregation of the platinum complexes is disrupted, leading to hyperchromism of the absorption bands. Once the aggregation is disrupted, and the concentration of DNA is sufficiently high, the normal hypochromic shifts can be observed.

While the initial hypochromism of the platinum complexes in aqueous solution prevents us from obtaining a precise determination of the binding constants to DNA, we can use the spectral data in acetonitrile to obtain a rough estimate of the absorption intensities of the unbound unaggregated forms. Using these data, we obtain complex−DNA binding constants in 20 mM sodium phosphate, 50 mM NaCl, pH 7.0, of $6 \times 10^3\ M^{-1}$ for $[(CN_2\text{-np})Pt(mes')_2]Cl_2$, $1 \times 10^4\ M^{-1}$ for both $[(np)Pt(mes')_2]Cl_2$ and $[(dppz)Pt(mes')_2]Cl_2$, and $2 \times 10^4\ M^{-1}$ for $[(CN\text{-np})Pt(mes')_2]Cl_2$. These values are comparable or slightly lower than those for other platinum(II) intercalators previously studied with complex−DNA binding constants in the range of $10^4-10^7\ M^{-1}$.[7b,9,32,33]

It is noteworthy that hypochromicity is not observed upon titration of DNA into a solution of complex **5** (20 μM). Indeed, there is little change in absorptivity of this complex even as the DNA concentration is increased to 1500 μM. Likely **5** shows different binding with DNA because it contains the smaller and less polar bp ligand, limiting deep intercalation into the DNA π stack.

Emission Spectra. For all the platinum complexes under study, only **3** is weakly emissive at ambient temperatures in

(30) Yam, V. W. W.; Wong, K. M. C.; Zhu, N. *J. Am. Chem. Soc*. **2002**, *124*, 6506−6507.
(31) Rüba, E.; Hart, J. R.; Barton, J. K. *Inorg. Chem.* **2004**, *43*, 4570−4578.
(32) McCoubrey, A.; Latham, H. C.; Cook, P. R.; Rodger, A.; Lowe, G. *FEBS Lett*. **1996**, *380*, 73−78.
(33) Howe-Grant, M.; Lippard, S. J. *Biochemistry* **1979**, *18*, 5762−5769.

Table 2. Ground-State and Estimated Excited-State Redox Potentials[a] of Pt(II) Complexes **1**−**5**

	E_{ox}[b] (V)	E_{red} (V)	E_{0-0} (eV)	E_{red}*[c] (V)	E_{ox}*[d] (V)
[(dppz)Pt(mes′)$_2$]Cl$_2$ (**1**)	1.36	−0.87	2.30 (540 nm)[e]	1.43	−0.94
[(np)Pt(mes′)$_2$]Cl$_2$ (**2**)	1.31	−1.27	2.26 (550 nm)[e]	0.99	−0.95
[(CN-np)Pt(mes′)$_2$]Cl$_2$ (**3**)	1.35	−0.99	2.12 (585 nm)[e]	1.13	−0.79
[(CN$_2$-np)Pt(mes′)$_2$]Cl$_2$ (**4**)	1.34	−0.57	<1.9 (>650 nm)[e]	<1.3	>−0.6
[(bp)Pt(mes′)$_2$]Cl$_2$ (**5**)	1.33	−1.27	>2.3 (<560 nm)[e]	>1.0	<−1.0

[a] Potentials are reported versus NHE ($Cp_2Fe^{+/0}$ = 0.66 V vs NHE). Uncertainties are ∼0.1 V. [b] E_{ox} values are taken from irreversible oxidation waves and therefore are estimates. [c] $E_{red}^* = E_{0-0} + E_{red}$. [d] $E_{ox}^* = E_{ox} - E_{0-0}$. [e] Wavelength of the 0−0 band in the structured emission spectra of these complexes in glassy 10 M LiCl solutions (complex concentrations ≈ 1×10^{-5} M; λ_{ex} = 350 nm) at 77 K. These values have an uncertainty of ±10 nm.

a degassed CH_3CN solution with an emission maximum of 620 nm. Upon titration of **3** (20 μM) with a DNA 20-mer in 20 mM sodium phosphate, 50 mM NaCl, pH 7.0, little emission is detected as the DNA concentration is increased to 660 μM; a weak emission band slowly develops upon further addition of the DNA 20-mer and reaches its maximum intensity at a DNA concentration of ∼2000 μM. The emission profile as a function of DNA titration thus parallels the hypochromic changes observed in the absorption experiment. This behavior provides additional evidence for Pt(II) complex aggregation in aqueous solution in competition with intercalation into the DNA π stack. No detectable emission is observed with other Pt(II) complexes upon DNA titration.

Complexes **1**−**5** are highly emissive at 77 K in 10 M LiCl glassy solutions when excited at 350 nm. The 0−0 band can be easily identified from these structured emission spectra (see Supporting Information for spectra and Table 2 for listed data) and reveal the triplet energies for these complexes.

Cyclic Voltammetry. Oxidation and reduction cyclic voltammograms for complexes **1**−**5** are shown in Figure 3, and the data are listed in Table 2. All of these compounds exhibit a single irreversible oxidation wave at ∼1.3 V versus NHE, which is substantially higher than that reported for a dppz complex of platinum containing unmodified mesityl ligands (0.98 V versus NHE),[22] presumably because of the electron-donating effects of the methyl substituents of mesityl and the electron-withdrawing effects of the quarternized ammonium substituents of the mes′ in complexes **1**−**5**. On the other hand, the first reduction potentials for complexes **1**−**5** (Figure 3 and Table 2) show a clear trend of CN_2-np > dppz > CN-np > np ≈ bp in the range of −0.5 to −1.3 V versus NHE. It is evident that complex **4**, with the most electron deficient diimine ligand (i.e., the CN_2-np ligand), exhibits the most positive reduction wave, while complex **2**, with the most electron-rich diimine ligand (i.e., the np ligand), exhibits the most negative reduction wave. This is consistent with the fact that the first reduction wave of the np ligand is 750 and 1070 mV more negative than that of the dppz and the CN_2-np ligand, respectively.[22] The HOMO and LUMO of these complexes depend on the metal center and the diimine ligand, respectively.

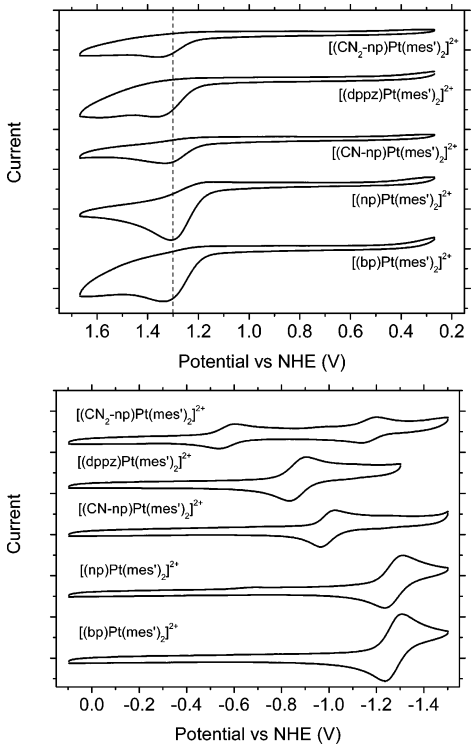

Figure 3. Oxidation (top) and reduction (bottom) cyclic voltammograms of the Pt(II) complexes in 0.1 M Bu_4NPF_6 in acetonitrile. Scan rate 100 mV s^{-1}, glassy carbon electrode.

Excited-State Redox Potentials. The combination of E_{0-0} data estimated from glassy emission spectra and ground-state redox potentials provided by the cyclic voltammetry permits the calculation of excited-state redox potentials for the Pt(II) complexes (Table 2). The excited-state reduction and oxidation potentials of complexes **1**−**5** are in the range of 1.0 to 1.5 and −0.6 to −1.0 V versus NHE, respectively, for one-electron reactions. Hence, these Pt(II) complexes serve as relatively strong excited-state oxidants and reductants.

Photoreactivity with d^{Cp}G and ^{Cp}C. Because the platinum complexes appear to be potent photooxidants and photoreductants, we tested their abilities to promote the oxidation of the cyclopropyl-modified nucleoside N^2-cyclopropyldeoxyguanosine (d^{Cp}G) and reduction of the cyclopropyl-modified nucleoside N^4-cyclopropylcytidine (^{Cp}C) upon photoactivation. The modified bases d^{Cp}G and ^{Cp}C are kinetically fast charge traps that can be incorporated into a DNA duplex.[15,16] Since electrochemical potentials measured for the nucleosides are all irreversible, the first oxidation and reduction potentials of ^{Cp}C can only be estimated to be >1.6 and −0.8 V versus NHE, respectively. The first oxidation potential of d^{Cp}G is ∼1.2 V versus NHE. Furthermore the solvent dependence of these potentials, as well as those for the Pt complexes, makes quantitation of the free energies for reactions with the DNA bases and within the DNA duplex even more difficult. Nonetheless, we estimate that complexes **1**, **2**, and **5**, with photoactivation, should be energetically sufficient to reduce ^{Cp}C; for **3** and **4**, the energies determined, given the uncertainties, are perhaps near those required for reduction. With respect to photooxidation,

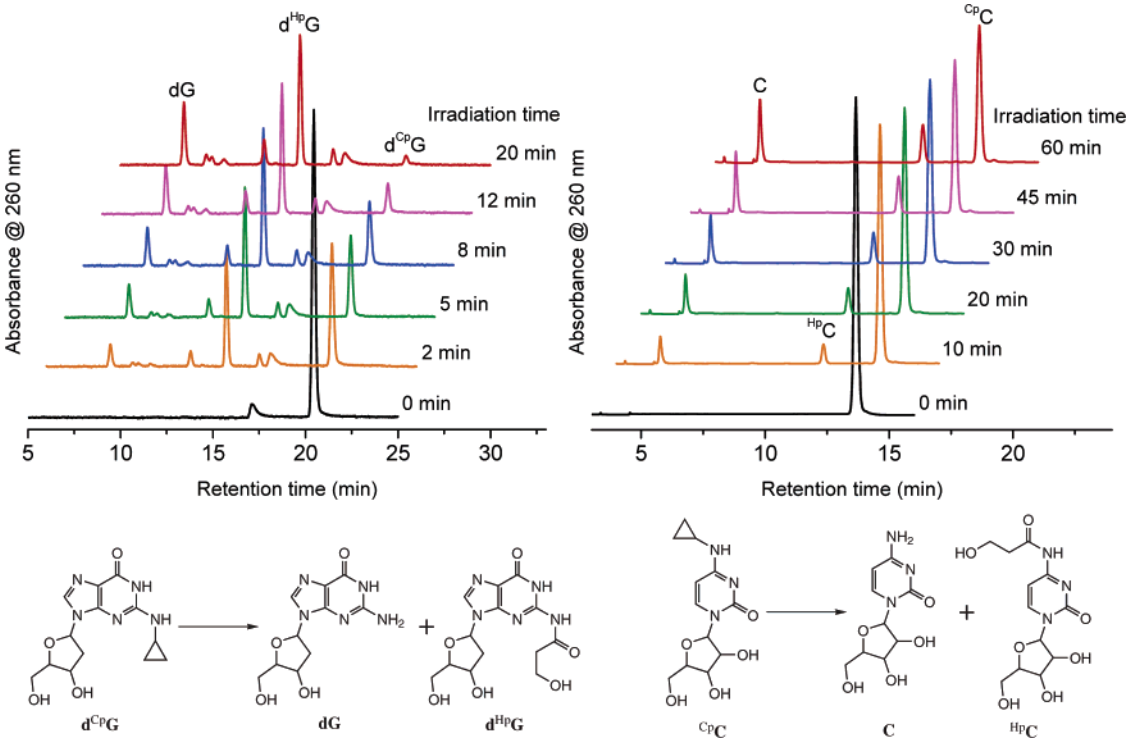

Figure 4. HPLC traces for photoreaction of d ^{Cp}G (left) and ^{Cp}C (right) nucleosides in the presence of $[(dppz)Pt(mes')_2]^{2+}$, **1**. Reaction conditions: 30 μL aliquot; 50 mM NaCl, 20 mM sodium phosphate, pH 7.0; 370 nm (~12.5 mW); for d ^{Cp}G, 20 μM d^{Cp}G, 20 μM Pt(II) complex; for ^{Cp}C, 500 μM ^{Cp}C, 500 μM Pt(II) complex. Products of photooxidation of d ^{Cp}G and photoreduction of ^{Cp}C nucleoside in the presence of Pt(II) complexes (bottom).

complexes **1**, **4**, and possibly **3** should be sufficient to oxidize d^{Cp}G by electron transfer; none should be capable of oxidizing ^{Cp}C upon photoactivation. It is noteworthy also that these diimine Pt(II) complexes are potentially sensitizers of singlet oxygen; thus, the oxidation of d^{Cp}G through a singlet-oxygen route must also be considered.

Figure 4 shows the HPLC analysis of products of photoreactions of the cyclopropylamine-substituted nucleosides with $[(dppz)Pt(mes')_2]^{2+}$, **1**. Figure 5 summarizes the results for all of the Pt complexes. As is evident in Figure 4, with photoactivation, some decrease in ^{Cp}C is observed with the appearance of two new peaks. At the concentration utilized, however, the decomposition of ^{Cp}C is not complete after 60 min of irradiation at 370 nm. Nevertheless, the two major products of this photoreaction can be isolated by collecting and concentrating the HPLC fractions. Mass spectroscopy reveals these products to be cytidine (C) (MW = 243) and (N^4-hydroxypropanoyl)cytidine (^{Hp}C) (MW = 315), and HPLC analysis using authentic compounds confirms the identifications. It should be noted that no reaction is detected upon irradiation at 370 nm in the absence of the Pt(II) complexes or in the presence of the Pt(II) complexes without light.

Interestingly, the products we observe with irradiation in the presence of the Pt complexes are identical to those observed upon the analogous photooxidation of ^{Cp}C or ^{Cp}G by a variety of photooxidants.[15,16] It is perhaps not surprising that in water the products of radical anion formation on the cyclopropyl ring resembles that for radical cation formation. We attribute the reactivity here to photoreduction, however, since none of the complexes are sufficiently potent for photooxidation of ^{Cp}C.

For comparison, the HPLC analysis of the photooxidation of d^{Cp}G by $[(dppz)Pt(mes')_2]^{2+}$ is also given in Figure 4. The complete decomposition of d^{Cp}G is found as a function of irradiation and two major products deoxyguanosine, dG, and (N^2-hydroxypropanoyl)deoxyguanosine, d^{Hp}G, are obtained. However it should be noted that additional oxidative products in low quantity are produced, and these may be associated with the singlet-oxygen reaction.

Figure 5 shows the reactivity with ^{Cp}C for all the complexes. On the basis of the photooxidation potentials, one would expect the reaction efficiency to decrease for $[(bp)Pt(mes')_2]^{2+} > [(dppz)Pt(mes')_2]^{2+} \approx [(np)Pt(mes')_2]^{2+} > [(CN\text{-}np)Pt(mes')_2]^{2+}$. Yet, we observe that $[(dppz)Pt(mes')_2]^{2+}$ is the most reactive, with some activity seen also for $[(CN\text{-}np)Pt(mes')_2]^{2+}$, but little if any reaction with other complexes. We ascribe this deviation to the differing binding abilities of the complexes with ^{Cp}C in solution. It is understandable that the np complex might be too hydrophobic, aggregating more on its own than with the substituted pyrimidine. For the bp complex, which is highly polar, no stacking interaction with ^{Cp}C would be expected. The lack of any photoreactivity seen earlier between silyl-protected pyrimidines and Pt(II)diimine bis(acetylide) complexes likely may also be ascribed to poor association in solution.[6c]

It is interesting that all of the Pt(II) complexes promote some decomposition of d^{Cp}G. The products obtained are dG and d^{Hp}G, along with lower concentrations of products we could not identify (Figure 4). The reaction efficiencies, given in Figure 5, follow the order $[(dppz)Pt(mes')_2]^{2+} > [(CN\text{-}$

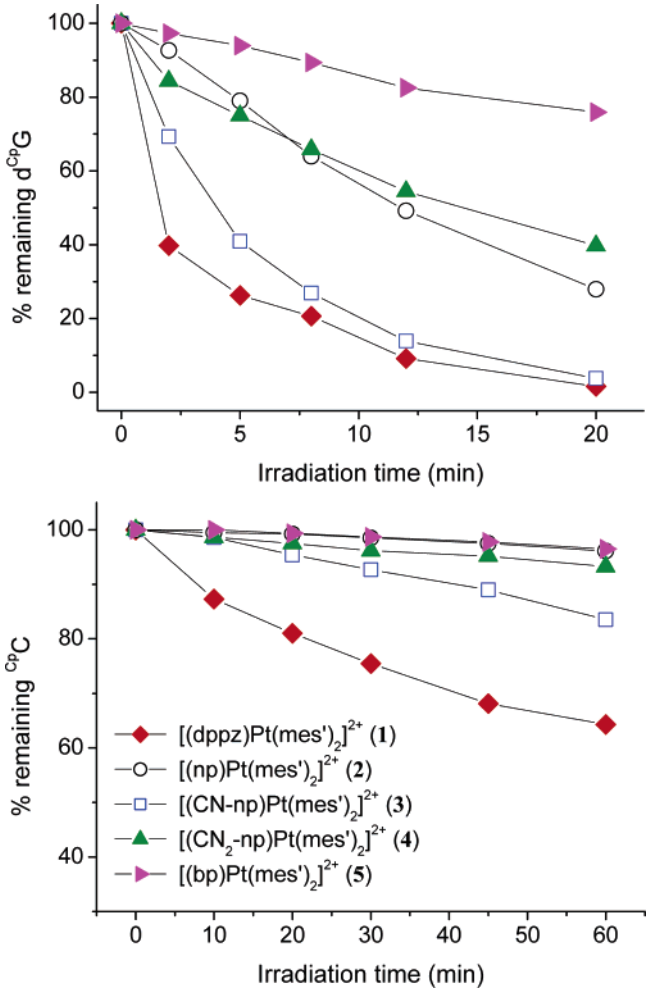

Figure 5. Photodecomposition of d^{Cp}G (top) and ^{Cp}C (bottom) nucleosides in the presence of Pt(II) complexes. Conditions: 30 μL aliquot in 50 mM NaCl, 20 mM sodium phosphate, pH 7.0; 370 nm (~12.5 mW) [330 nm (~9 mW) for [(bp)Pt(mes′$_2$)]Cl$_2$]; for d^{Cp}G, 20 μM d^{Cp}G, 20 μM Pt(II) complex; for ^{Cp}C, 500 μM ^{Cp}C, 500 μM Pt(II) complex.

np)Pt(mes′)$_2$]$^{2+}$ > [(CN$_2$-np)Pt(mes′)$_2$]$^{2+}$ ≈ [(np)Pt(mes′)$_2$]$^{2+}$ > [(bp)Pt(mes′)$_2$]$^{2+}$. This order of reactivity more closely parallels the order of the photoreduction potentials, although here too, modulations in efficiencies because of the differential associations of the complexes with d^{Cp}G are seen. Perhaps, most notable is that there is any reaction of the np complex with d^{Cp}G. Here, the self-aggregation of the complex may enhance singlet-oxygen formation, and with ^{1}O$_2$ as an intermediate, similar oxidation products of d^{Cp}G would be expected. Indeed, some singlet-oxygen-sensitized reaction for all the complexes cannot be ruled out; irradiation of a mixture of **1**, TEMP, and O$_2$ in buffer yields a strong EPR triplet for TEMPO radical (Supporting Information).

Photoreduction and Photooxidation of DNA Duplexes. We have also examined the photoreaction of [(dppz)-Pt(mes′)$_2$]$^{2+}$ (**1**) with various DNA duplexes. This complex was shown most effectively to both photoreduce ^{Cp}C and photooxidize d^{Cp}G (vide supra). Furthermore, the binding of a variety of metal complexes containing the dppz ligand to DNA by intercalative stacking is well established;[9,20,27] the importance of intercalative stacking for efficient DNA-mediated oxidation has been demonstrated,[10] and a similar

Table 3. DNA Duplexes Examined

	DNA duplex
G/C	5′-ACG ATT GAC CGA GTC AT-3′ 3′-TGC TAA CTG GCT CAG TA-5′
G/^{Cp}C	5′-ACG ATT GAC CGA GTC AT-3′ 3′-TGC TAA ^{Cp}CTG GCT CAG TA-5′
I/^{Cp}C	5′-ACG ATT IAC CGA GTC AT-3′ 3′-TGC TAA ^{Cp}CTG GCT CAG TA-5′
^{Cp}G/^{Cp}C	5′-ACG ATT ^{Cp}GAC CGA GTC AT-3′ 3′-TGC TAA ^{Cp}CTG GCT CAG TA-5′
^{Cp}G/C	5′-ACG ATT ^{Cp}GAC CGA GTC AT-3′ 3′-TGC TAA CTG GCT CAG TA-5′

sensitivity to base-pair stacking for DNA-mediated photoreduction is anticipated. It should be noted, however, that since the Pt complex binds to DNA noncovalently, these experiments do not establish DNA-mediated hole or electron transfers over the long range; instead these experiments provide the foundation and characterization for subsequent quantitative comparisons as a function of distance and sequence. To test DNA photoreactivity, several duplexes (**G/C**, **G/^{Cp}C**, **I/^{Cp}C**, **^{Cp}G/C**, and **^{Cp}G/^{Cp}C**) annealed from five 17-mer single strands were prepared (Table 3).

Figure 6 shows the results for reactions with DNA duplexes in the presence and absence of O$_2$. Solutions of Pt(II) complex (5 or 50 μM) and DNA duplex (5 μM) were irradiated (370 nm, ~9 mW, for **1** or 330 nm, ~6 mW, for **5**) followed by enzymatic digestion and HPLC analysis. We examined first the reactions with DNAs containing no modified bases (Figure 6a). After 1 h, **1** at 50 μM yields 25% damage to G and 10% to C in duplex **G/C**, while T and A are unaffected. Energetically, the triplet excited state of **1** is sufficient to oxidize G but not C; the oxidation potentials of dG and dC nucleosides are estimated to be 1.3 and >1.6 versus NHE, respectively.[8] Likely the complex has a photoreduction potential also in the range for the reduction of dC. Thus, irreversible oxidative damage to guanine is expected, since the guanine radical is long-lived and yields several irreversible products. Reaction with cytosine could certainly reflect reductive damage, although the cytosine radical anion is not similarly reactive, and rapid charge recombination would be favored.

Since d^{Cp}G and d^{Cp}C have been demonstrated to be effective irreversible kinetic traps for DNA redox chemistry, DNAs containing these modified bases provide more sensitive substrates to test for oxidative and reductive damage. Under aerobic conditions, the Pt complex (50 μM) is found to decompose both d^{Cp}C and d^{Cp}G in duplexes **G/^{Cp}C** and **^{Cp}G/^{Cp}C** (Figure 6b and c). It is noteworthy that the decomposition rate of d^{Cp}G is much higher than that of d^{Cp}C. Also, ~60% of G is consumed after 1 h.

To assay for singlet-oxygen-sensitized damage, we also examined the reactions in D$_2$O, where ^{1}O$_2$ is longer lived. In D$_2$O, we find that the damage of d^{Cp}G and d^{Cp}C remains unchanged. However, G damage is somewhat enhanced (data

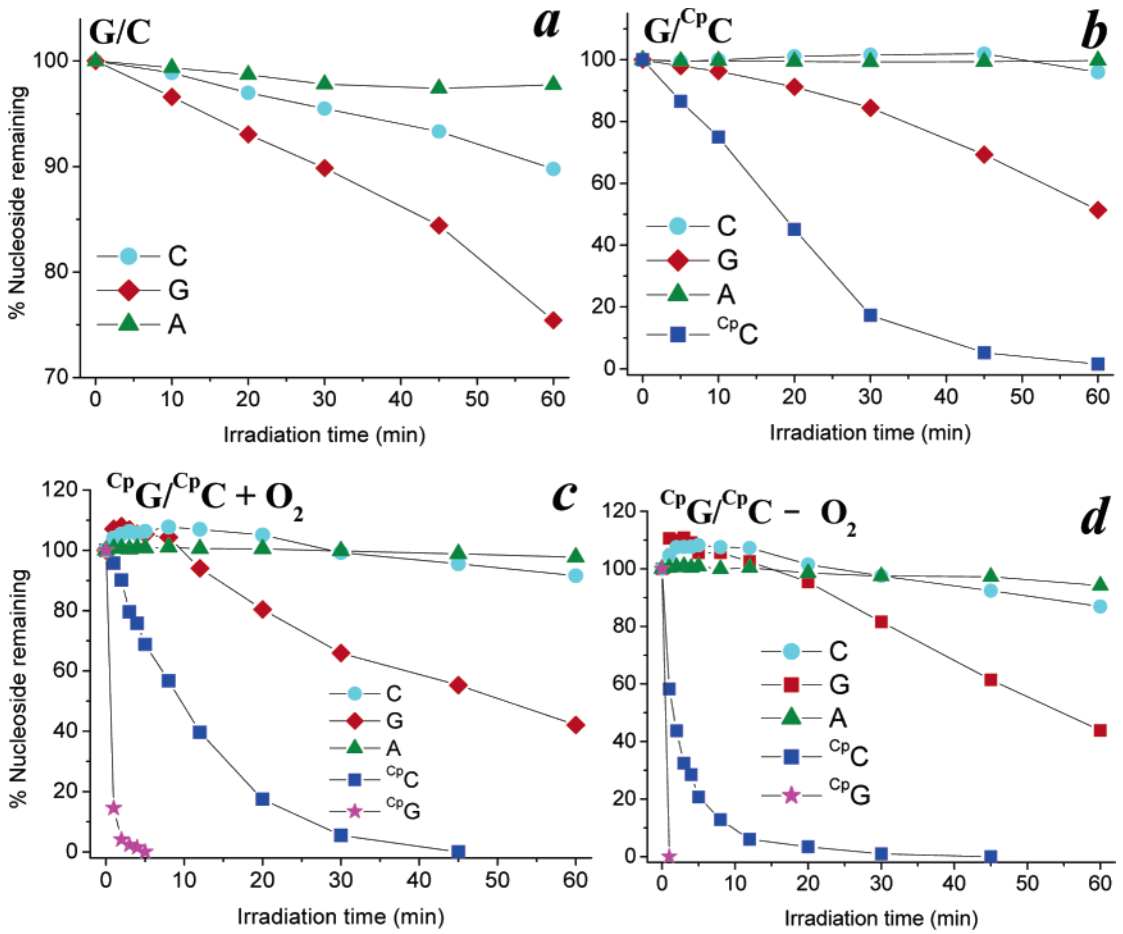

Figure 6. Photoreaction of $[(dppz)Pt(mes')_2]^{2+}$, **1**, with DNA duplexes. Plots show percent nucleoside remaining after photoreaction in 50 mM NaCl, 20 mM sodium phosphate, pH 7.0, of 50 μM **1** with 5 μM duplex **G/C** (with O_2, a), **G/^{Cp}C** (with O_2, b), and **^{Cp}G/^{Cp}C** (with O_2, c, without O_2, d), and after nuclease digestion and HPLC analysis. For HPLC quantitation, T was used as internal standard.

not shown). Thus, some background singlet-oxygen reaction with G may occur; singlet-oxygen reactions promoting ring opening are not expected, however.

We have also examined photoreactions under anaerobic conditions to focus purely on electron- or hole-transfer chemistry (Figure 6d). It is interesting that here, without oxygen, the decompositions of both ^{Cp}G and ^{Cp}C are actually accelerated compared to aerobic environments, while decomposition of G is diminished. These variations with O_2, therefore, indicate that, in part, there is a competition between energy and electron/hole-transfer pathways, where electron/hole transfers are favored in the absence of O_2.

To further compare and contrast the photoreduction and photooxidation chemistry, we also examined the effects of complementary bases on d^{Cp}G and d^{Cp}C decomposition by **1** at 5 μM. As is evident in Figure 7a and b, we find that the decomposition of d^{Cp}C remains constant (or slightly less) when its complementary base is switched from G to I. In comparison, we have seen for photooxidations that damage is enhanced with I versus G, which we have attributed to less competition for hole localization.[15,16] The lack of enhancement of reaction with inosine substitution therefore further supports our assignment of photoreduction chemistry here for d^{Cp}C.

Significantly, the decomposition of d^{Cp}C diminishes when its complementary base is d^{Cp}G versus G (Figure 7b and c). Surely, d^{Cp}G is a more effective hole trap than G, and this more effective oxidation trap, d^{Cp}G, reveals the competition between electron trapping by d^{Cp}C and hole trapping by d^{Cp}G. In fact, the decomposition of d^{Cp}G is unaffected by C or ^{Cp}C as complementary base (Figure 7c and d). Thus, hole trapping by d^{Cp}G must be more effective than electron trapping by d^{Cp}C in these duplexes.

Summary and Implications. Thus, we have developed a group of water soluble Pt(II) complexes with extended π-conjugated α-diimine ligands that exhibit unique excited-state redox properties, and these redox properties can be utilized in probing *both* oxidation and reduction reactions on DNA. In particular, $[(dppz)Pt(mes')_2]^{2+}$ binds the DNA duplex and can serve both as a potent photooxidant and photoreductant. Once excited, the complex is found oxidatively to decompose d^{Cp}G and reductively to decompose ^{Cp}C, the kinetically fast reporters of charge transfer. Moreover, within the DNA duplex modified with these charge traps, the triplet excited state of the Pt(II) intercalator is seen to promote DNA electron transfer as well as DNA hole transfer. In fact, with the Pt complex, hole trapping by d^{Cp}G is found to be more effective than electron trapping by d^{Cp}C. Therefore, using these powerful cyclopropylamine charge traps and the DNA-bound Pt complex, we can now begin directly to compare and contrast hole and electron transport through DNA.

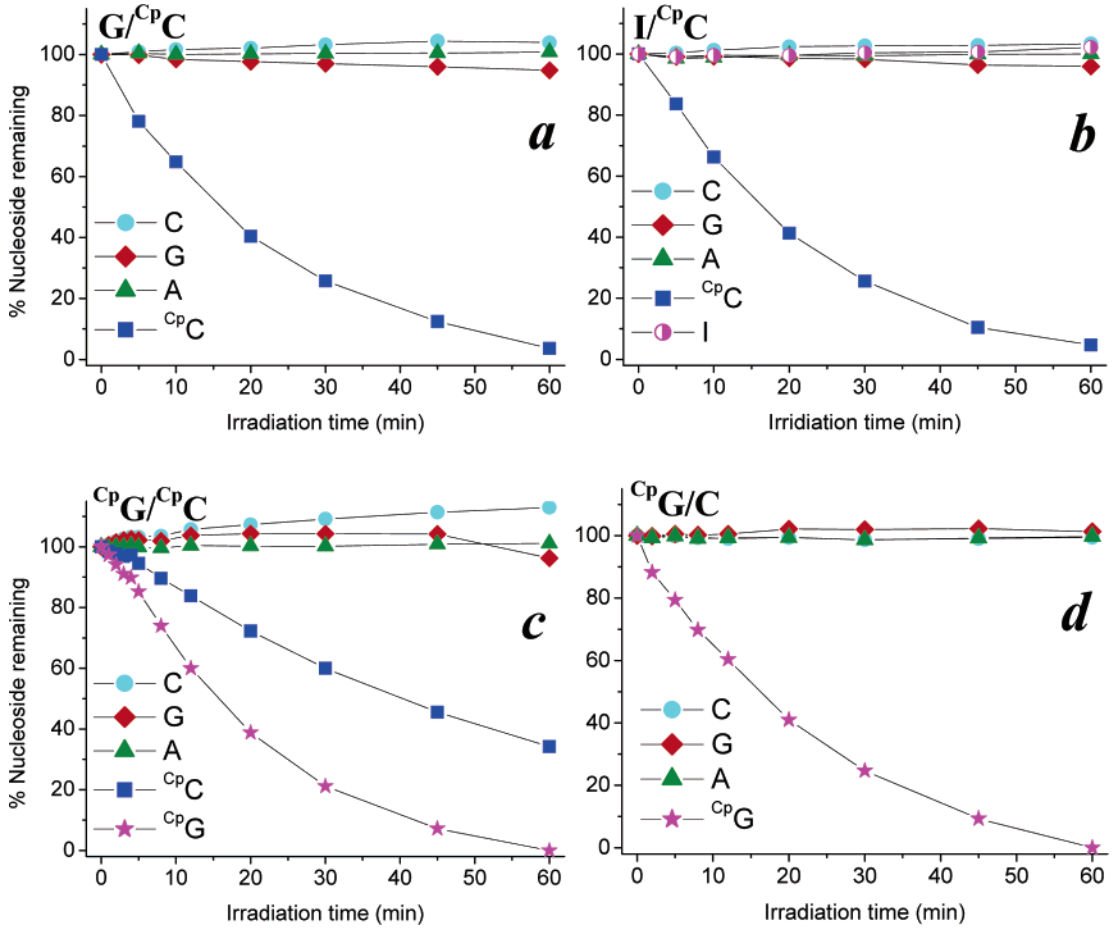

Figure 7. Photoreaction of $[(dppz)Pt(mes')2]^{2+}$, **1**, with DNA duplexes with variations in base modifications. Plots show percent nucleoside remaining after photoreaction of 5 μM **1** and 5 μM duplex **G/^{Cp}C** (a), **I/^{Cp}C** (b), **^{Cp}G/^{Cp}C** (c), and **^{Cp}G/C** (d) in the presence of O_2, and after nuclease digestion and HPLC analysis. For HPLC quantitation, T was used as internal standard.

Acknowledgment. We are grateful to the NIH (GM33309) for financial support, the Distinguished Research Award of Prof. Chi-Ming Che at The University of Hong Kong for a postdoctoral fellowship (W.L.), and the American Cancer Society for a postdoctoral fellowship (D.A.V.). We also thank Lawrence M. Henling at the Caltech X-ray Crystallography Laboratory for help with structure determinations, and Dr. Eylon Yavin for helpful discussions.

Supporting Information Available: Scheme depicting the synthesis of the ligands, glassy emission spectra, CIF file, and structural parameters of crystal structure of **2**·$(DMF)_3$·$(H2O)_2$, additional figures of the UV−vis traces of the Pt(II) complexes upon DNA titration, and HPLC traces for photoreactions with ^{Cp}C, d^{Cp}G, and DNAs. This material is available free of charge via the Internet at http://pubs.acs.org.

IC051124L